ONR TECHNICAL REPORT No. 97
Project: NR 056-678
Contract: Nonr 3357(01)

DYNAMIC X-RAY DIFFRACTION FROM POLYETHYLENE

by

T. Kawaguchi, T. Ito, H. Kawai, D. Kevdy and R. S. Stein
Polymer Research Institute
University of Massachusetts
Amherst, Massachusetts

November 1967

145

DYNAMIC X-RAY DIFFRACTION FROM POLYETHYLENE*

T. Kawaguchi†, T. Ito‡, H. Kawai‡, D. Keedy and R. S. Stein
Polymer Research Institute
University of Massachusetts
Amherst, Massachusetts

Abstract

The technique of dynamic x-ray diffraction is described in which the periodically varying diffracted x-ray intensity is analyzed for a sample of a polymer film subjected to a periodic strain. The intensity change may be resolved into a real part, $\Delta I'$, varying in-phase with the strain and an imaginary out-of-phase component, $\Delta I''$. This resolution is carried out for the amorphous scattering and the diffraction from the {110} and {200} planes of medium density polyethylene at 30°C and at frequencies between 0.02 and 1.25 HZ. $\Delta I'$ decreases with frequency and $\Delta I''$ increases with frequency in the range as a consequence of a crystal orientation process having a relaxation time of the order of 1 sec. Measurements at temperatures of 30°, 45°, and 60°C produce a frequency shift associated with an activation energy of 25 Kcal/mole which is close to that for the α_2 process studied mechanically. By integrating the ΔI values over azimuthal angle it is possible to determine the real and imaginary parts of the dynamic orientation function, $\Delta f'$ and $\Delta f''$.

---

*Supported in part by a contract with the Office of Naval Research and in part by grants from the Army Research Office, the Petroleum Research Fund, and the Monsanto Corporation.

†Present Address: Toyo Rayon Company, Shiga, Japan.
‡Present Address: Kyoto Kogei Seni University, Kyoto, Japan.
‡Present Address: Department of Polymer Chemistry, Kyoto University, Kyoto, Japan.

Introduction

Studies of the rheo-optical properties of polyethylene have demonstrated a time-dependent optical response to strain. When a sample is deformed, there is an immediate orientation change followed by a slower change This latter change may be revealed by measurements of the increase in birefringence during relaxation at constant length, or by the frequency dependence of the strain-optical coefficient during vibration[1,2]. This is believed to be primarily a result of a two-stage crystal orientation process. The first step is a rapid orientation accompanying the spherulite deformation, which is followed by a slower change in orientation within the deformed spherulite. Of course, the amorphous material also contributes to the birefringence, but it is thought that the crystal orientation change is the prime contributor, because (a) high density polyethylene shows a larger birefringence change than low density polyethylene, even though it has less amorphous material, and (b) the birefringence change is much too large to be accountable in terms of even a complete change in amorphous orientation from that of complete disorder to perfect orientation.

Thus, it is believed that the process of orientation of crystals in a crystalline high polymer takes a finite time and may occur in a number of ways such as interlamellae slip and crystal deformation involving intracrystalline migration of dislocations. The direct proof of this hypothesis is best accomplished by x-ray diffraction techniques. This is difficult, however, because of the times of seconds or less involved with these processes.

A method for x-ray study was described[3] in a previous "Letter" involving an x-ray "stroboscopic" technique illustrated in Fig. (1). The sample was vibrated in tension in the x-ray beam at frequencies from 0.01 to 30 cps with a dynamic amplitude of 2.5% superimposed on a static strain of the order of

22.5%. This 22.5% static strain was necessary in order that the sample remain taut during vibration. A detector was set at a Bragg angle of 21.6° corresponding to the 110 reflection. The preamplified output of the detector was distributed among four counting channels by a rotating cam which operated microswitches. Each channel was activated during a small part of the period of strain so that counts could be repetitively accumulated at a particular strain interval over many cycles of straining. Each channel accumulated counts during a different interval of strain. The diffracted intensity could then be compared for different parts of the strain cycle. It was found that at low frequencies, the change in diffracted intensity with strain was essentially the same as that found during a static experiment whereas differences appeared at straining frequencies of the order of 10-20 cps. The effect was small, however, but the results indicated that crystal orientation times for the medium density polyethylene studied were of the order of 0.1 sec. in agreement with the birefringence results.

In an effort to improve the precision of the study, two modifications in technique were made:

(a) The mechanical commutator was replaced by an optical commutator in which a rotating sector synchronized with the sample stretching intercepted the light beam falling on a bank of four photocells which drove gating circuits such that when light fell on a photocell the corresponding counting circuit was activated. The program of activation of scalers was determined by the pattern cut out on the rotating sector. This arrangement was not limited by the finite time of operation of the cam and microswitches of the mechanical commutator.

(b) Rather than accumulating counts over only a small interval of the strain cycle, a given channel would accumulate over a larger part of the strain cycle and the integrated intensities over different parts of the strain cycle

would be compared. This technique is capable of giving a measurement of both the real and the imaginary parts of the crystal orientation - strain coefficient as described in the "Theory" section.

The Photoswitch Commutator

Details of the new "photo-switch" commutator are shown in Fig. (2). The "shaft in phase with sinusoidal strain" is identical with the shaft bearing the cams for the mechanical commutator of the original apparatus. The light from the bulb (an automobile headlamp) is collimated into a vertically elongated rectangle focused on the chopper disc by a cylindrical lens and mirror. The chopper disc contains four sector windows corresponding to the four counting channels. These have a common center at the shaft axes and are spaced at different distances along the radius so as to interrupt the light falling on four phototubes located in back of the disc. The sector windows are of angular width corresponding to the fraction of the time a given counting channel is to be activated and are located at an angular position corresponding to the phase angle between the strain and the time that the corresponding counting channel is to be activated. A separate chopping disc is made for each counting program.

The outputs of the phototubes are passed through parallel channels of a Heathkit Operational amplifier (EUW19A) and pulse shaping circuits and Zenner diodes serving as gates for the amplified geiger tube outputs to the scalers (Berkely Model 2000). A portion of one of these outputs is fed to another scaler for counting shaft rotations to serve as a measure of the sample vibration frequency. In this manner, the output of the geiger counter may pass to a given scaler only during the time when the light beam passes through the corresponding chopping disc window. The signal to the counter is therefore controlled without having the time delay introduced by a mechanical switch and camshaft. The response time is limited only by the time constants of the electronic circuits.

The "photoswitch commutator" may be calibrated by feeding a constant frequency signal (from a signal generator) through the gating circuit (instead of the geiger tube signal) and determining the "switch constant," S_k, which is the fraction of the entire vibration period that a given counting channel is activated. When making an actual measurement, the scaler reading would then be divided by its S_k in order to determine counting rate. S_k was found to remain constant to within $\pm$ 1% over times comparable with measurements and to be independent of the frequency of sample vibration. Examination of the signals with a dual beam oscilloscope has verified that no phase differences are introduced by the electronics.

Data Reduction[4]

The diffracted intensity is given by

$$I_{diff} = (I_{total} - I_{back})\, k_{pol} \cdot k_{abs} - I_{incoh} \qquad (1)$$

where

I_{diff} = corrected diffracted intensity

I_{total} = total (measured) diffracted intensity

k_{pol} = polarization correction factor

$$= 2/[1 + \cos^2 (2\theta)] \qquad (2)$$

for filtered radiation

k_{abs} = absorption correction factor

$$= [\exp (\mu d \sec\theta)]/\left(\frac{d_o}{d} \sec\theta\right) \qquad (3)$$

where d and μ are the sample thickness and d_o is the initial thickness and absorption coefficient.

I_{incoh} = incoherent scattering intensity

I_{back} = background intensity

The vibrating samples is subjected to a periodic strain, $\lambda(t)$ given by

$$\lambda(t) = \lambda_o - \Delta\lambda \cos \omega t \tag{4}$$

where λ_o is the static tensile strain, $\Delta\lambda$ is the dynamic strain amplitude, and ω is the angular frequency of vibration.

The vibrating sample gives a vibrating diffracted intensity given by

$$I_{diff} = I_o - \Delta I_{diff} \cos (\omega t - \chi) \tag{5}$$

where I_o is the static diffracted intensity at strain λ_o and I_{diff} is the amplitude of the periodic variation in intensity which lags the strain by phase angle χ. This may also be expressed using complex notation giving

$$I_{diff} = I_o - \Delta I'_{diff} \cos \omega t - \Delta I''_{diff} \sin \omega t \tag{6}$$

where

$$\Delta I'_{diff} = \Delta I_{diff} \cos \chi \tag{7}$$

is the component of ΔI_{diff} which is in-phase with the strain, and

$$\Delta I''_{diff} = \Delta I_{diff} \sin \chi \tag{8}$$

is the component which is out-of-phase.

It should be remembered that when the sample is vibrated, its thickness, d, will also vary periodically with amplitude Δd.

$$d(t) = d_o + \Delta d \cos (\omega t - \delta_d) \tag{9}$$

It is assumed that the thickness changes in phase with the length ($\delta_d = 0$). If the volume of the sample is conserved and the strain is uniaxial

$$\Delta d = -\left(\Delta\lambda/2\right) d_o \tag{10}$$

This corrected thickness must be used in the correction factors to obtain the true diffracted intensity per unit volume of sample.

The diffracted intensity at a particular Bragg angle θ results from overlapping peaks contributed by different crystal planes. The intensities were assumed to be linearly additive.

$$I_{diff}(\theta, \phi) = \Sigma c_j(\theta, \phi) I^o_j(\phi) \tag{11}$$

where $I^{o}_{j}(\phi)$ is the contribution of the diffraction from the j^{th} crystal plane to the diffraction at Bragg angle, θ, and azimuthal angle ϕ. For unoriented samples, $I^{o}_{j}(\theta, \phi)$ is independent of ϕ, but for oriented samples, its variation with ϕ is dependent upon the orientation distribution of the crystals.

$c_j(\theta, \phi)$ is a shape factor which is assumed to be given by a Lorenzian type equation

$$c_j(\theta, \phi) = \frac{1}{1 + [\theta - \theta^{o}_{j}(\phi)]^2 / B_j(\phi)^2} \qquad (12)$$

$\theta^{o}_{j}(\phi)$ is the angle at which the diffraction maximum of the j^{th} peak occurs and is dependent upon the interplaner spacing. If one makes the fairly good assumption that the crystal spacings are independent of orientation, then θ^{o}_{j} will be independent of ϕ. $B_j(\phi)$ is a measure of the width of the diffraction peak from the j^{th} plane which depends upon crystal size and perfection. Since both size and perfection are known to change upon crystal orientation, it is best to permit $B_j(\phi)$ to depend upon ϕ. The use of a computer program to determine the c_j's has been described[5]. An example of such resolution of the observed diffraction peak from a low density polyethylene sample into contributions from the amorphous (110) and (200) peaks is shown in Fig. (3). For a sample stretched 22.5%. The contributions from background intensity and incoherent scattering are also shown on this figure. It is necessary to carry out such a resolution for each value of ϕ.

In this work, it is assumed that $\Delta I'$ and $\Delta I''$ may be resolved into contributions from component peaks using the same coefficients. This is

$$\Delta I'_{diff}(\theta, \phi) = \sum_j c_j(\theta, \phi)\, \Delta I'_j(\phi) \qquad (13)$$

and

$$\Delta I''_{diff}(\theta, \phi) = \sum_j c_j(\theta, \phi)\, \Delta I''_j(\phi) \qquad (14)$$

This assumption implies that the fractional contribution of the change in orientation of each crystal plane to the change in diffracted intensity at a given angle is proportional to the fractional contribution which the diffraction from that plane makes to the static diffracted intensity. Of course this is not necessarily so, but may be tested by making diffraction measurements before and after a static change in strain $\Delta\lambda$. In this case, the phase angle, χ, is zero so $\Delta I'' = 0$, and only Eq. (13) may be tested. Such a check indicates that the assumption is valid at least for this zero frequency experiment, but does not assure that it is true at higher frequencies.

Semi-Circular Sector Technique[4]

In order to obtain $\Delta I'$ and $\Delta I''$ from experimental data, the "semi-circular sector" technique was devised which is capable of giving greater precision than the previously described small angle sector techniques. Rather than having each counting channel activated for only a small interval (10° of phase) of the sample vibration period, the rotating sector of the photoswitch is constructed so that the counting channel is activated during 1/2 or 180° of the straining cycle. These period are staggered in phase so that the first sector is activated in the interval between 0 and π, the second between π and 2π, the third from $\pi/2$ to $3\pi/2$, and the fourth from $-\pi/2$ to $\pi/2$. By comparing the accumulated counts over many cycles of vibration during these intervals, it is possible to obtain $\Delta I'$ and $\Delta I''$.

Consider the case of a sample vibrating with a period T for n cycles of vibration occurring in a time interval $\tau = n\,T$. The accumulated count for the first channel is

$$N_{0-\pi}(\tau) = n\int_0^{T/2} I(2\theta, \phi)\,dt$$

$$= n\int_0^{T/2} [I^\circ - \Delta I \cos(\omega t + \chi)]dt$$

$$= \frac{nT}{2}[I^\circ - (2/\pi)\,\Delta I \sin\chi] \qquad (15)$$

The average intensity (measured in units of counts/sec.) is then

$$I_{0-\pi} = N_{0-\pi}(\tau)/(1/2)\tau = I^\circ - (2/\pi)\,\Delta I \sin\chi \qquad (16)$$

χ is the phase angle between the strain and the diffracted intensity at particular diffraction angles, 2θ and ϕ.

Similarly, for the other counting channels

$$I_{\pi-2\pi} = I^\circ + (2/\pi)\,\Delta I \sin\chi \qquad (17)$$

$$I_{\pi/2-3\pi/2} = I^\circ - (2/\pi)\,\Delta I \cos\chi \qquad (18)$$

and

$$I_{(-\pi/2)-\pi/2} = I^{o} + (2/\pi)\,\Delta I \cos\chi \tag{19}$$

From these it is apparent that[4]

$$I^{o} = [N_{0-\pi} - N_{\pi-2\pi}]/\tau$$

$$= [N_{\pi/2-3\pi/2} - N_{(-\pi/2)-\pi/2}]/\tau \tag{20}$$

$$\Delta I' = \Delta I \cos\chi$$

$$= [N_{(-\pi)-\pi} - N_{\pi/2-3\pi/2\pi}]/2\tau \tag{21}$$

$$\Delta I'' = \Delta I \sin\chi$$

$$= \pi[N_{\pi-2\pi} - N_{0-\pi}]/2 \tag{22}$$

Thus from measurements of the counts of the four scalers, $N_{0-\pi}$, $N_{\pi-2\pi}$, $N_{\pi/2-3\pi/2}$, and $N_{(-\pi)-\pi}$, it is possible to obtain I_o, $\Delta I'$ and $\Delta I''$.

An analysis of errors[4] which may be introduced into the above procedure due to small errors in the time of starting and finishing a count for each channel indicates that a better procedure involves measuring the counts both when the apparatus is driven in the forward and the reverse direction[4], and suitably averaging the results.

Sample Preparation

Samples were prepared from an experimental Monsanto medium density polyethylene identical with that used in other experiments in this laboratory[7]. Films were molded with a laboratory press at 160°C using a 0.5 mm thick spacer between aluminum foil and copper sheets. After 10 minutes in the press, they were quenched in a dry-ice-ethanol bath. The films were then remolded using the same press conditions but a thinner spacer (0.3 mm) and quenching in an ethanol-dry ice bath. X-ray examination of samples prepared in this manner revealed no orientation.

MEASUREMENTS OF STATIC DIFFRACTION

The dependence of the total diffracted intensity upon azimuthal angle is shown in Fig. (4) at the 2θ corresponding to the peaks of the {110} and {200} scattering at elongations of 20% and 25%. The variation of intensity in the dynamic experiment at 2.5% strain amplitude about the static strain of 22.5% is within this small interval between the 20% and 25% static curves. It is the study of this small difference which is the purpose of this work. The {200} diffraction concentrates at the equator, while the {110} diffraction concentrates at a ϕ of 20 - 30° from the equator. The difference in intensity ΔI between the static 20% and 25% curves is shown in Fig. (5) as a function of azimuthal angle. At small azimuthal angles, ΔI is positive, representing an increase of number of diffracting crystal with strain, whereas at larger azimuthal angles ΔI is negative representing a decrease in number of diffracting

crystals. Thus the change of intensity which is observed in the dynamic experiment represents a change in orientation of the diffracting crystals rather than a change in number of crystals. For small strains, ΔI is found to vary linearly with strain so that a sinusoidal variation of strain produces a sinusoidal variation of the diffracted intensity (as is required by the theoretical analysis). This is demonstrated in Fig. (6) in which the intensity of the {110} peak is measured as the strain is varied in a stepwise fashion between 20% and 25%. It is expected that during dynamic vibration, the diffracted intensity also changes sinusoidally in this manner. However, the amplitude of the intensity change depends upon the frequency and temperature, and the intensity is no longer in phase with the strain but is shifted through the phase angle χ.

Dynamic Diffraction Measurements

When the sample was vibrated, part of the mechanical energy was converted into heat resulting in a temperature rise. This could be avoided by circulation of air over the sample, in which case the diffraction by the sample was independent of the time during which the sample was vibrated.

For example, the result of the measurement of $\Delta I'_{total}$ and $\Delta I''_{total}$ for the {110} peak at 30°C at different azimuthal angles at frequencies between 0.02 and 1.25 Hz. is shown in Fig. 7. In accordance with the static results, $\Delta I'_{total}$ is positive at $\phi = 20°$ but is negative at the higher azimuthal angles. The absolute values decrease with increasing frequency. $\Delta I''_{total}$ increases in absolute value with increasing frequency as a result of the increasing phase angle between the diffracted intensity change and the strain. The phase angle itself could be obtained from the relationship

$$\tan \chi_{total} = \frac{\Delta I''_{total}}{\Delta I'_{total}} = \frac{\Delta I_{total} \sin \delta_{total}}{\Delta I_{total} \cos \delta_{total}} \qquad (23)$$

The measured intensities were corrected for background, incoherent scattering, polarization, and absorption using Eqs. (1), (2), and (3). The curves were resolved into amorphous, {110} and {200} contributions as in Fig. (3) for each azimuthal angle.

After these corrections and resolutions, the resulting frequency dependence of $\Delta I'$ and $\Delta I''$ for the {110} and {200} peaks are given in Figs. (8) and (9). The trends are the same as for the uncorrected intensities where the absolute values of $\Delta I'_k$ is positive at small azimuthal angles and negative at large corresponding to a tendency for these planes to orient equatorially with strain. The tangents of the phase angles between the variation of the diffracted intensity and strain for the corrected {110} and {200} peaks are plotted as a function of frequency in Figs. (10) and (11). These are negative at all frequencies characteristic of the diffracting intensity variation lagging strain. The phase lag is small at 0.02 Hz. but increases with frequency.

It is seen from Figs. (10) and (11) that the frequency dependence of the loss tangent is dependent upon azimuthal angle, being greater for the smaller azimuthal angles. This indicates that the ability of the more highly oriented crystals to follow higher frequency strains is less than that for more poorly oriented crystals. This may be consistent with the postulate that the more highly oriented crystals are larger and more perfect, and consequently less mobile.

Amorphous Orientation

Plots of the azimuthal angle variation of $\Delta I'_{am}$ and $\Delta I''_{am}$ for the corrected amorphous orientation are given in Fig. (12). This is independent of frequency and may be compared with the azimuthal angle variation of $\Delta I'_k$ and $\Delta I''_k$ for the corrected {110} and {200} peaks in Figs. (13) and (14). The variation of $\Delta I'_{am}$ is only about 1/8 that of the {110} peak indicating a degree of amorphous orientation change that is compatible with the amount of amorphous orientation estimated by such methods as birefringence and sonic modulus. The lack of frequency dependence of $\Delta I'_{am}$ and the negligible value of $\Delta I''_{am}$ is significant. This shows that the variation in amorphous orientation is in phase with the strain at all frequencies at least to within the precision of $\pm$ 25% for the measurement of the small volume of $\Delta I'$ possible here. It is not likely that this observed variation is an artifact arising from the lack of complete separations of overlapping crystalline peaks, since such contributions would be frequency dependent and would make an observable contribution to $\Delta I''_{am}$.

The difference in dynamic behavior of the amorphous scattering and that of crystalline diffraction favors the postulate of there being a distinct amorphous phase in this comparatively low crystallinity sample rather than the amorphous scattering arising from distributed defects within the crystalline phase. In the latter case, if the crystalline diffraction was frequency dependent and lagged the strain in phase, it would be expected that the included amorphous defects would exhibit similar frequency dependence.

Determination of Dynamic Orientation Function

The state of orientation of the (hkl) plane of a crystal is often conveniently described by the Hermans orientation function[7,8]

$$f_{hkl} = [3\langle \cos^2 \alpha_{hkl} \rangle - 1]/2 \qquad (24)$$

where α_{hkl} is the angle between the normal to the {hkl} crystal plane and the principal axis of strain. $\langle \cos^2 \alpha \rangle$ may be determined from the diffracted intensity by

$$\langle \cos^2 \alpha_j \rangle = \frac{\int_0^{\pi} \sin^2 \phi \, I_j(\phi) \cos\phi \, d\phi}{\int_0^{\pi} I_j(\phi) \cos\phi \, d\phi} \tag{25}$$

where the incident x-ray intensity falls on the sample at an angle θ_j to the film normal.

It is recalled that f_{hkl} is a measure of the state of orientation of the {hkl} plane and ranges from + 1 when the normal to the plane is parallel to the strain direction to - 1/2 when the normal is perpendicular to this direction. For random orientation, $f_{hkl} = 0$.

When the sample is strained periodically, the orientation function will oscillate periodically at the straining frequency, and its change may be resolved into a real and imaginary part.

$$f_j = f^o_j - \Delta f'_j \cos \omega t - \Delta f''_j \sin \omega t \tag{26}$$

where f^o_j, $\Delta f'_j$ and $\Delta f''_j$ are the orientation function of the static strain and for the portion of the change in orientation function varying in-phase and out-of-phase with the strain, respectively. It may be shown[4] that these may be given by

$$f_j^{\circ} = \frac{1}{2}\left[3\,\frac{I_j^{11}}{I_j^{21}} - 1\right] \tag{27}$$

$$\Delta f_j' = \frac{3}{2}\,\frac{I_j^{11}}{I_j^{21}}\left[\frac{I_j^{12}}{I_j^{11}} - \frac{I_j^{22}}{I_j^{21}}\right] \tag{28}$$

and

$$\Delta f_j'' = \frac{3}{2}\,\frac{I_j^{11}}{I_j^{21}}\left[\frac{I_j^{13}}{I_j^{11}} - \frac{I_j^{23}}{I_j^{21}}\right] \tag{29}$$

where the I_j^{kl} terms are integrals over the azimuthal angle, ϕ, defined by

$$I_j^{11} = \int_0^{\pi/2} \sin^2\phi\; I^{\circ}_j\,(\phi)\,\cos\phi\; d\phi \tag{30}$$

$$I_j^{12} = \int_0^{\pi/2} \sin^2\phi\; \Delta I'_j\,(\phi)\,\cos\phi\; d\phi \tag{31}$$

$$I_j^{13} = \int_0^{\pi/2} \sin^2\phi\; \Delta I''_j\,(\phi)\,\cos\phi\; d\phi \tag{32}$$

$$I_j^{21} = \int_0^{\pi/2} I_j^{\circ}\,(\phi)\,\cos\phi\; d\phi \tag{33}$$

$$I_j^{22} = \int_0^{\pi/2} \Delta I'_j (\phi) \cos\phi \, d\phi \qquad (34)$$

$$I_j^{23} = \int_0^{\pi/2} \Delta I''_j (\phi) \cos\phi \, d\phi \qquad (35)$$

These integrals may be evaluated numerically using the experimental values of I^o_j, $\Delta I'_j$ and $\Delta I''_j$ evaluated as a function of ϕ.

The values of $\Delta f'_{110}$, $\Delta f''_{110}$, $\Delta f'_{200}$ and $\Delta f''_{200}$ obtained in this way are plotted as a function of frequency in Fig. (15). The in-phase components, $\Delta f'_k$ are negative indicating that the {110} and {200} plane normals tend to orient perpendicularly to the direction of strain upon increasing the strain. The magnitude of $\Delta f'_k$ decreases with increasing frequency indicating that less orientation of these crystal planes occurs at higher frequency. The out-of-phase components $\Delta f''_k$ increase in magnitude with increasing frequency. This corresponds to a negative phase angle between the orientation function change and the strain, again indicating that the crystal orientation lags strain by an increasing amount with increasing frequency.

From these values of $\Delta f'_k$ and $\Delta f''_k$ it is possible to calculate the crystalline contribution to the real and imaginary strain-optical coefficient K' and K". This is discussed elsewhere[9] where it is shown that the crystalline contribution can account for most of the observed strain-optical coefficient.

Temperature Dependence

A temperature control chamber was constructed for the dynamic x-ray diffraction apparatus which permitted circulating heated air about the sample. Temperatures could be maintained to $\pm$ 1°C in the range of 25°C to 150°C. Prior

to measurement the sample was mechanically conditioned by vibrating at 10 Hz. for one hour at 60°C. The variation of $\Delta I'_{total}$ and $\Delta I''_{total}$ (uncorrected) with frequency for the {110} peak at $\phi = 90°$ are given in Fig. (16) at 30°C, 45°C, and 60°C. It is apparent that the decrease in $\Delta I'_{total}$ and increase of $\Delta I''_{total}$ occurs at higher frequency at higher temperature, the change occurring at about 0.2 Hz., 0.8 Hz. and 7 Hz. at 30°C, 45°C and 60°C respectively. A plot of the logarithm of this frequency (where the out-of-phase component reaches a value of 1 count/sec.) against the reciprocal of absolute temperature is given in Fig. (17). These points give a straight line with a slope giving an apparent activation energy of 25Kcal/mol., a value also found from the temperature dependence of dynamic birefringence[10].

Discussion of Results

Several investigators have reported[11,12,13] that the high temperature or α dispersion region of mechanical loss for polyethylene actually consists of two or more dispersions. Nakayasu[11], etc. al., reported "that the α dispersion could be decomposed into two mechanisms designated α_1 and α_2 with activation energies of 28 and 46 Kcal/mol., respectively." Takayanagi[14,15] found that for polyethylene single crystals, the lower temperature side of the α_c dispersion had an activation energy of 25 Kcal/mol. Hideshima[16] examined the effect of absorption of diluent and pointed out that this caused a shift in the α_1 dispersion toward lower temperatures while the α_2 dispersion is unaffected. Thereby, he concluded that the α_1 dispersion is related to the amorphous regions whereas the α_2 dispersion is concerned with processes within the crystals.

Studies by McCrum and Morris[17] on the α loss peak of high density polyethylene indicate two crystalline contributions which he designates α and α' for the low (70°C) and high (110°C) temperature components, respectively.

He attributes the α component to intracrystalline phenomona and the α' component to interlamella slip in contrast to the assignments of α_1 and α_2 by Takayanagi. The α' assignment is based upon the dependency of this peak upon anisotropy, irradiation, and crystallization temperature while the α peak has no dependency upon crystallization conditions. Activation energies of the order of 25 - 30 Kcal/mole were found for both of these peaks.

Illers[18] has reported mechanical relaxation studies on single crystals of the n-paraffins while Sinnott[19,20] has reported results of such studies on polyethylene single crystals. Sinnott reports a single α loss peak at a frequency which increases with annealing temperature (and crystal thickness) but with an area which decreases with annealing temperature. On the basis of this observation, he has assigned the α loss peak as being due to motion of the chain in the folds of single crystals.

In a recent review, Hoffman, Williams and Passaglia[21] have considered this data along with dielectric data and concluded that the α peak consists of two components, one of which decreases in area with increasing crystal thickness and is due to fold motion, while the other has an area independent of thickness and is related to a combined rotation-translation of chains within the crystals.

Recently, Takayanagi[22] has reported that for isothermally crystallized single crystals, a single α loss peak is observed with an area which increases with increasing growth temperature. He believes this to be related to rotational motion within the lattice and which represents the temperature at which the crystals become internally viscoelastic.

The studies reported here are not at present adequate to distinguish between the various proposals for the α peak but do require that it be associated with a process in which the orientation of the crystals reversibly changes with

vibration of the sample. Three possibilities might be considered. (1) The peak is the α' peak described by McCrum and is related to interlamella slip. (2) The peak is the component of the α peak described by Hoffman, Williams and Passaglia which is related to fold motion. This fold motion allows crystals to slip over each other more easily. (This does not seem too likely an explanation in view of the fact that our measurements were on polyethylene containing considerable amorphous material, residing principally in the interlamella regions and which would become mobile at the lower temperature of the β peak). (3) The x-ray dispersion corresponds to the component of the α peak at which motion within the crystal lattice becomes possible. This onset of intracrystalline motion itself would not be sufficient to account for the orientational change found by the dynamic x-ray and birefringence techniques. It is likely, however, as suggested by Takayanagi[21], that when internal motion commences, the crystal becomes viscoelastic and can undergo orientational changes more easily. In this way, the onset of internal motion is reflected in the increase in the dynamic orientation function with temperature.

It is desirable, in order to obtain better comparison with dynamic mechanical spectra, to determine the variation of the dynamic orientation function (as determined by x-ray diffraction) with temperature at a fixed frequency and to compare this result with the corresponding variation of dynamic birefringence and modulus. Such studies are presently in progress.

References

1. R. S. Stein, S. Onogi, K. Sasaguri and D. A. Keedy, J. Appl. Phys. 34, 80 (1963).
2. R. Yamada and R. S. Stein, J. Appl. Phys. 36, 3005 (1965).
3. H. Kawai, T. Ito, D. A. Keedy and R. S. Stein, J. Polymer Sci. B 2, 1075 (1964).
4. T. Kawaguchi, ONR Report No. 86, Project: NR 056-378, Contract: Nonr 3357(01), Polymer Research Institute, University of Massachusetts, Amherst, Massachusetts, April 1966.
5. C. R. Desper, ONR Technical Report No. 80, Project: NR 056-378, Contract: Nonr 3357(01), Polymer Research Institute, University of Massachusetts, Amherst, Massachusetts, October 1965.
6. S. Hoshino, J. Powers, D. G. LeGrand, H. Kawai and R. S. Stein, J. Polymer Sci. 58, 185 (1962).
7. J. J. Hermans, P. Hermans, D. Vermaos and A. Weidinger, Rec. Trav. Chim. 65, 427 (1946).
8. R. S. Stein, J. Polymer Sci. 31, 327 (1958).
9. T. Kawaguchi, I. Kimura, A. Takeuchi and R. S. Stein, J. Polymer Sci. B, 5, 339 (1967).
10. A. Takeuchi and R. S. Stein, J. Polymer Sci. A2, in press.
11. H. Nakayasu, H. Markovitz and D. J. Plazek, Trans. Soc. Rheology 5, 261 (1961).
12. S. Iwayanagi in Solid State Physics, edited by F. Seitz and D. Turnbull, Academic Press, New York, Vol. 14, p. 458, 1963.
13. Y. Wada and K. Tsuge, Japan. J. Appl. Phys., 1, 64 (1962).

References-2

14. M. Takayanagi, Proc. Fourth Int. Congress Rheology, Part I, E. H. Lee and A. L. Copley, Ed., Interscience, New York, 1965.

15. T. Aremaki, S. Minami, F. Nagatoshi and M. Takayanagi, Progress Polymer Physics [Japan, 7, 237 (1964)].

16. T. Hidashima, Progress Polymer Physics (Japan) 9, 279 (1966).

17. N. G. McCrum and E. L. Morris, Proc. Royal Soc. A292, 506 (1965).

18. K. H. Illers, Rheo. Acta 3, 202 (1964).

19. K. M. Sinnott, J. Appl. Phys. 37, 3385 (1966).

20. K. M. Sinnott, J. Polymer Sci. C, No. 14, 141 (1966).

21. J. C. Hoffman, G. Williams and E. Passaglia, J. Polymer Sci. C, No. 14, 173 (1966).

22. M. Takayanagi, private communication, 1967.

Figures

1. The dynamic x-ray diffraction apparatus.
2. The photoswitch commutator.
3. The resolution of the total equatorial scattering into contributions from the background, incoherent scattering, amorphous scattering and diffraction from the {110} and {200} planes.
4. The variation of I_{total} with azimuthal angle at 2θ values corresponding to the positions of the {110} and {200} diffraction at static strains of 20% and 25%.
5. The variation of ΔI (difference in scattered intensity between 25% and 20% static strain) with azimuthal angle at 2θ values corresponding to the positions of the {110} and {200} diffraction.
6. The change in total diffracted intensity at the position of the {110} peak at $\phi = 90°$ with strain as the strain is varied sinusoidally in a stepwise fashion between 20% and 25%.
7. The variation of $\Delta I'_{total}$ and $\Delta I''_{total}$ with frequency at the position of the {110} peak at different azimuthal angles at 30°C.
8. The variation of the corrected values of $\Delta I'_{110}$ and $\Delta I''_{110}$ with frequency for different azimuthal angles at a temperature of 30°C.
9. The variation of the corrected values of $\Delta I'_{200}$ and $\Delta I''_{200}$ with frequency for different azimuthal angles at a temperature of 30°C.
10. The variation of the loss tangent, $\tan \chi_{110}$, for the 110 peak with frequency at a number of azimuthal angles at 30°C.
11. The variation of the loss tangent, $\tan \chi_{200}$, for the 200 peak with frequency at a number of azimuthal angles at 30°C.
12. The variation of the variation of $\Delta I'_{am}$ and $\Delta I''_{am}$ for the corrected amorphous peak with azimuthal angle at 30°C.

Figures-2

13. The variation of the corrected $\Delta I'_{110}$ and $\Delta I''_{100}$ with azimuthal angle at a number of frequencies at 30°C.

14. The variation of the corrected $\Delta I'_{200}$ and $\Delta I''_{200}$ with azimuthal angle at a number of frequencies at 30°C.

15. The variation of $\Delta f'_{110}$, $\Delta f''_{110}$, $\Delta f'_{200}$ and $\Delta f''_{200}$ with frequency at 30°C.

16. The variation of $\Delta I'_{total}$ and $\Delta I''_{total}$ (uncorrected) with frequency at the position of the {110} peak at $\phi = 90°$ at temperatures of 30°C, 45°C and 60°C.

17. The variation of Log ν for the frequency at which $\Delta I''_{total}$ reaches 1 count/sec. with the reciprocal of the absolute temperature.

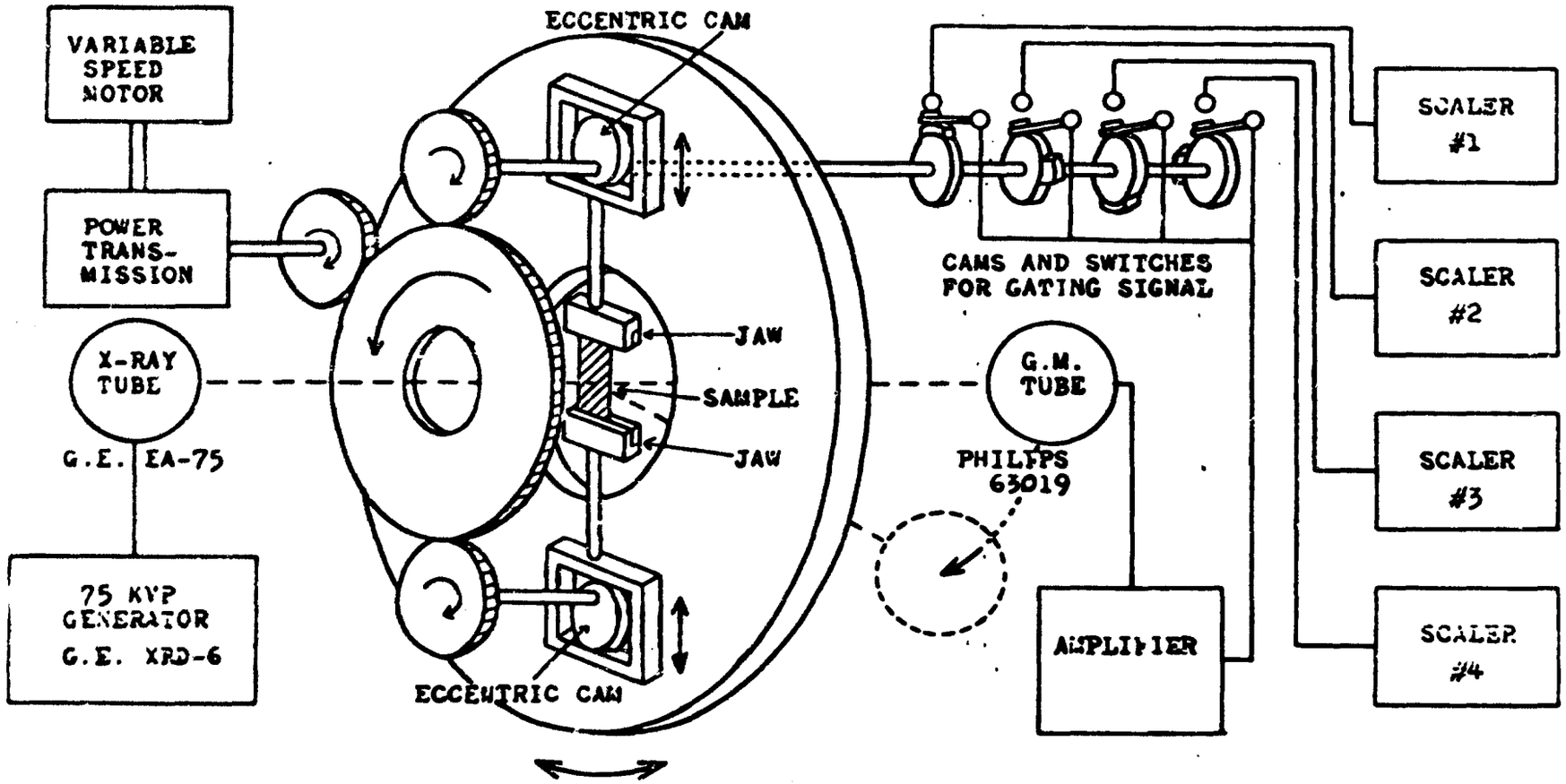
VARIABLE SPEED MOTOR
POWER TRANS-MISSION
X-RAY TUBE
G.E. EA-75
75 KVP GENERATOR G.E. XRD-6
ECCENTRIC CAM
JAW
SAMPLE
JAW
ECCENTRIC CAM
CAMS AND SWITCHES FOR GATING SIGNAL
G.M. TUBE
PHILIPS 63019
AMPLIFIER
SCALER #1
SCALER #2
SCALER #3
SCALER #4

FIGURE 1

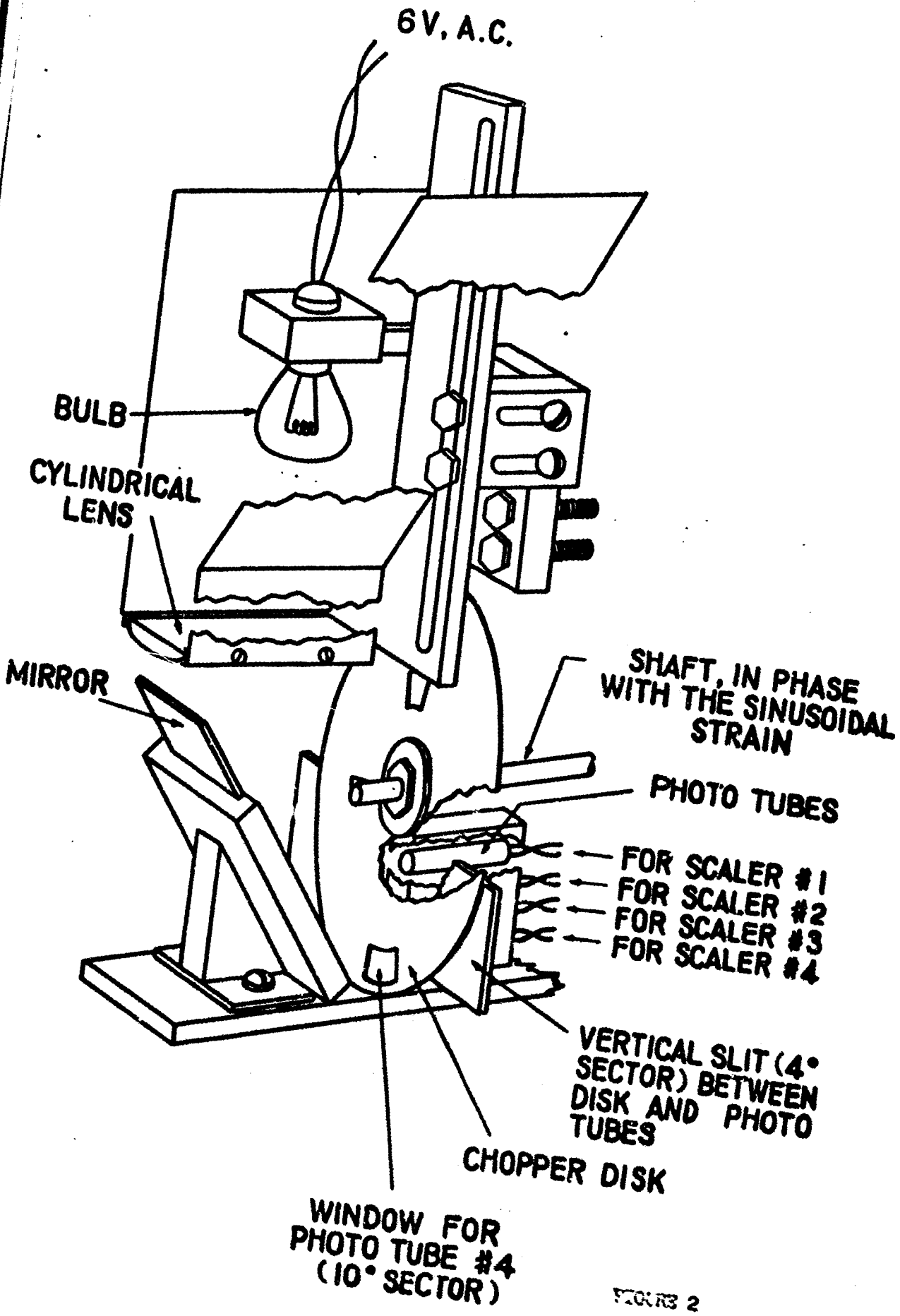
6V, A.C.
BULB
CYLINDRICAL LENS
MIRROR
SHAFT, IN PHASE WITH THE SINUSOIDAL STRAIN
PHOTO TUBES
FOR SCALER #1
FOR SCALER #2
FOR SCALER #3
FOR SCALER #4
VERTICAL SLIT (4° SECTOR) BETWEEN DISK AND PHOTO TUBES
CHOPPER DISK
WINDOW FOR PHOTO TUBE #4 (10° SECTOR)

FIGURE 2

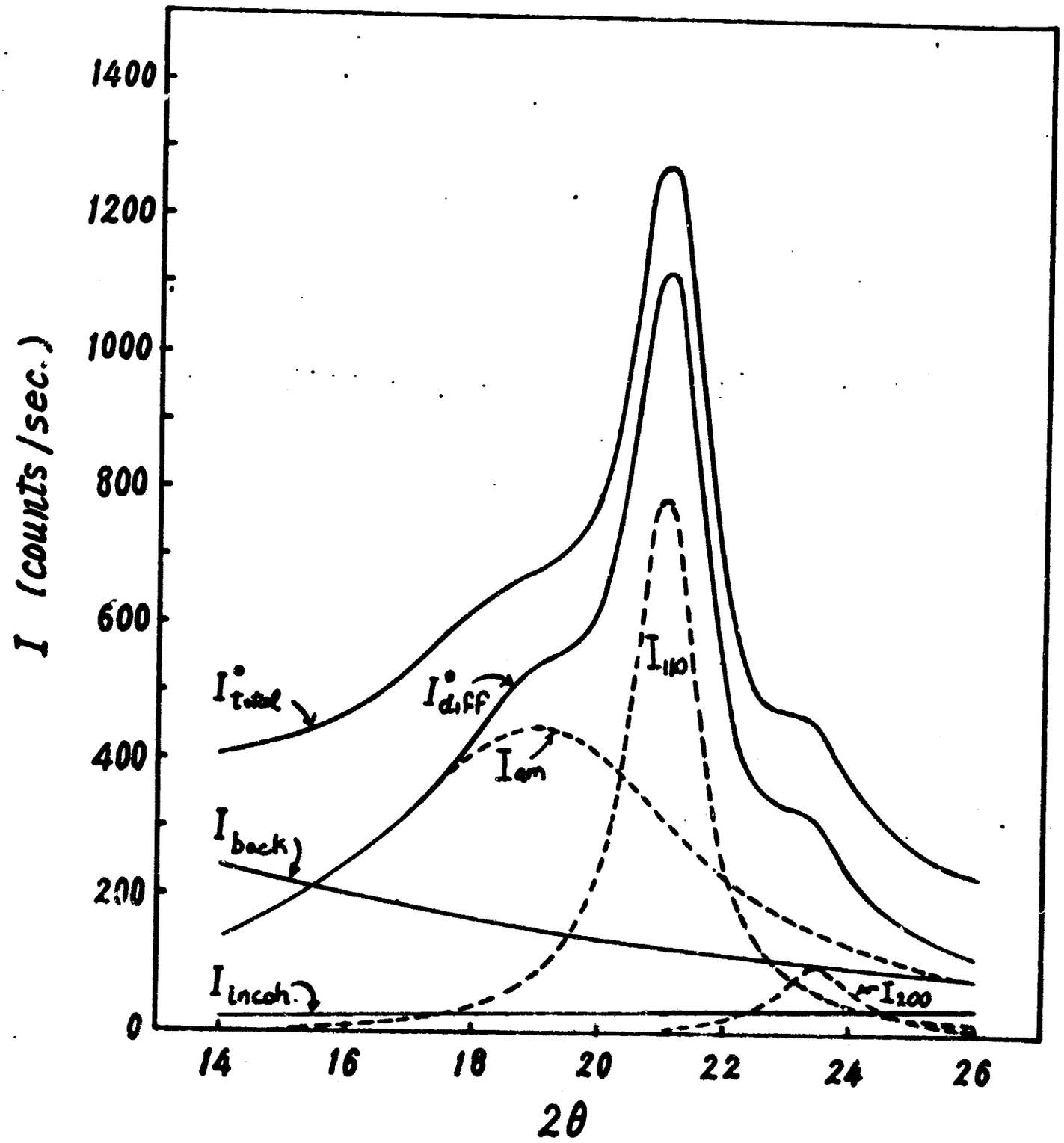
1400
1200
1000
800
600
400
200
0
I (counts/sec.)
14
16
18
20
22
24
26
2θ
$I^{\bullet}_{total}$
$I^{\bullet}_{diff}$
I_{110}
I_{am}
I_{back}
$I_{incoh.}$
I_{200}

FIGURE 3

FIGURE 4

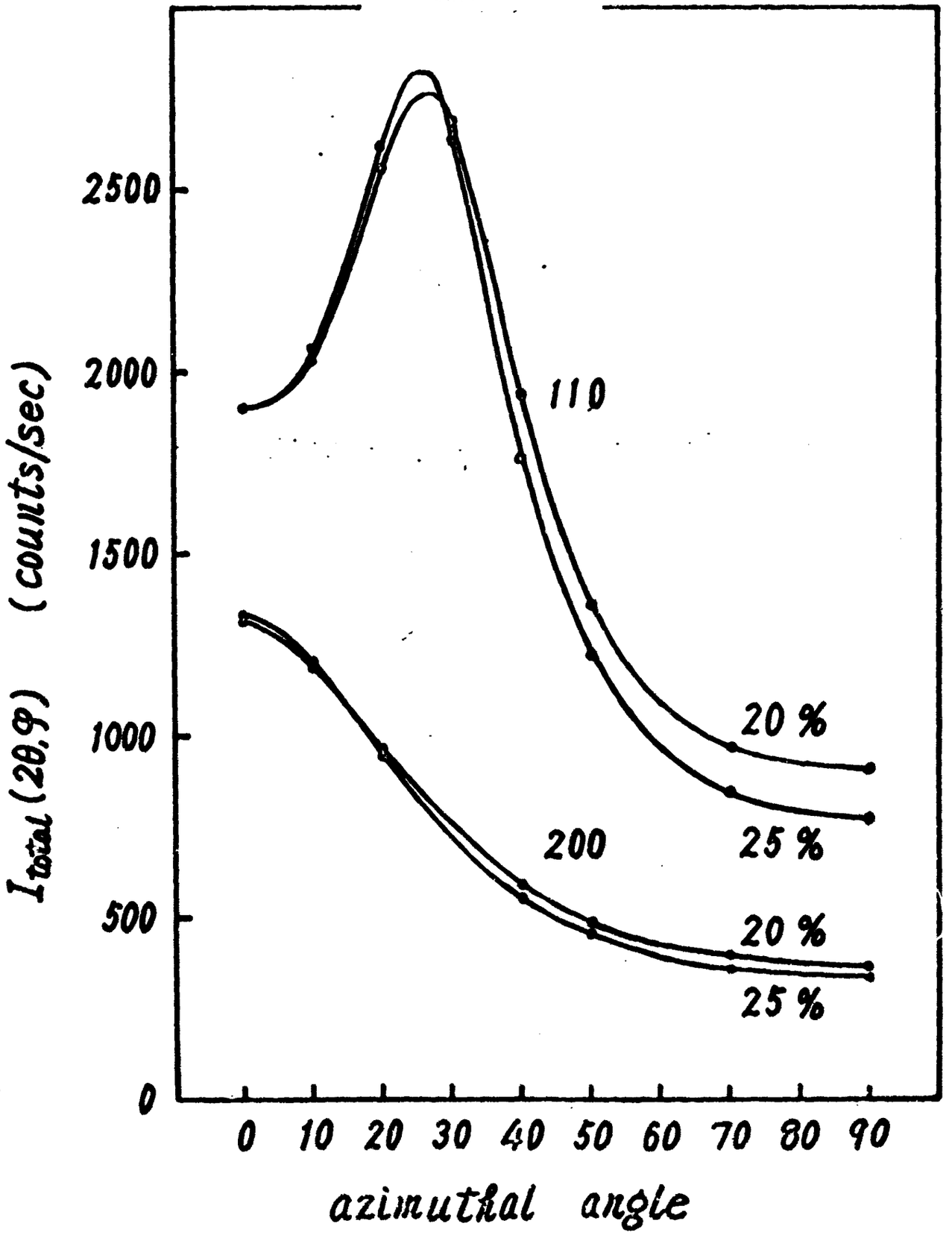
2500
2000
1500
1000
500
0
I_{total} (2θ,ψ) (counts/sec)
110
20 %
25 %
200
20 %
25 %
0 10 20 30 40 50 60 70 80 90
azimuthal angle

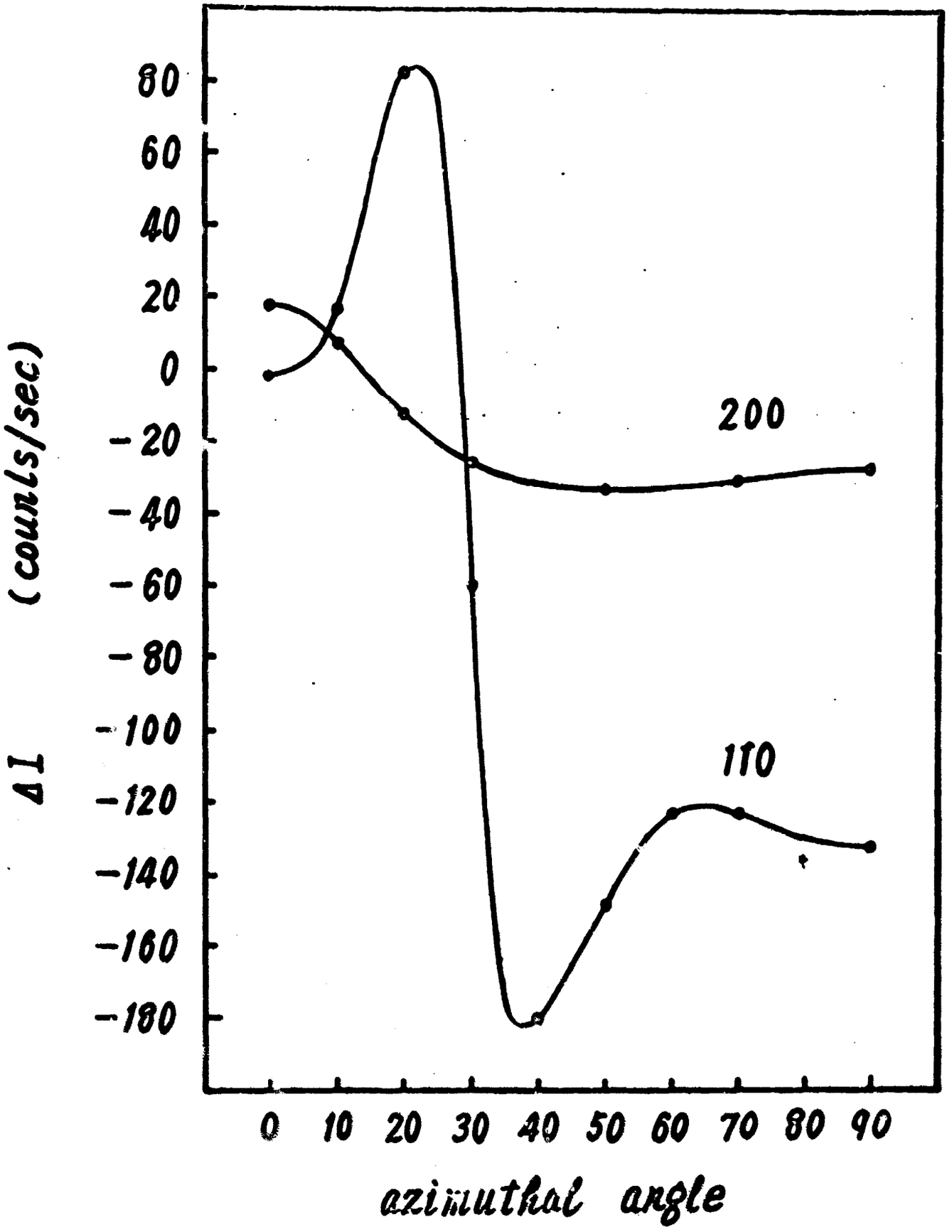
80
60
40
20
0
-20
-40
-60
-80
-100
-120
-140
-160
-180
ΔI (counts/sec)
200
110
0
10
20
30
40
50
60
70
80
90
azimuthal angle

FIGURE 5

FIGURE 6

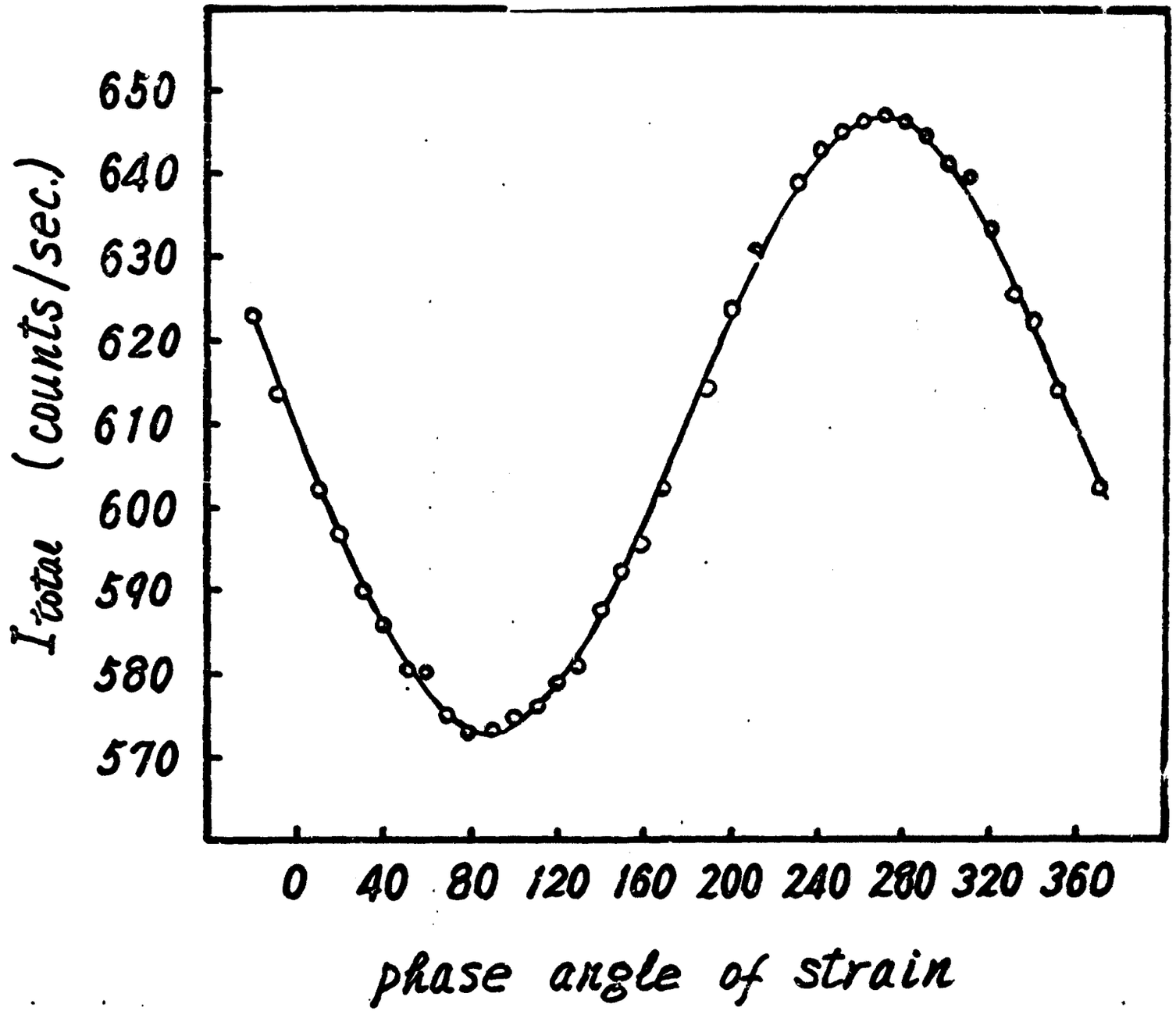
650
640
630
620
610
600
590
580
570
I total (counts/sec.)
0
40
80
120
160
200
240
280
320
360
phase angle of strain

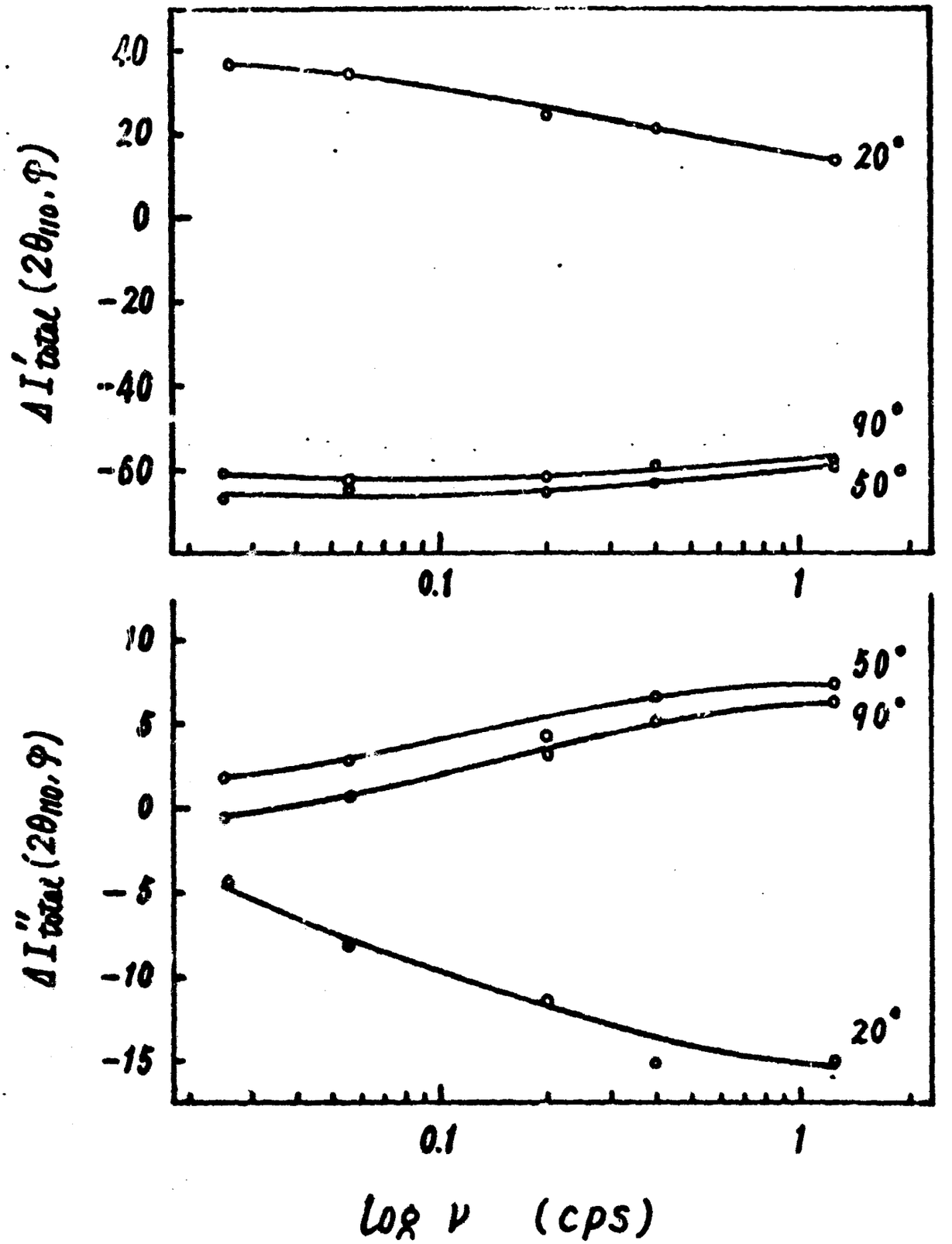
40
20
0
-20
-40
-60
$\Delta I'_{total}(2\theta_{110}, \varphi)$
20°
90°
50°
0.1
1
10
5
0
-5
-10
-15
$\Delta I''_{total}(2\theta_{110}, \varphi)$
50°
90°
20°
0.1
1
log ν (cps)

FIGURE 7

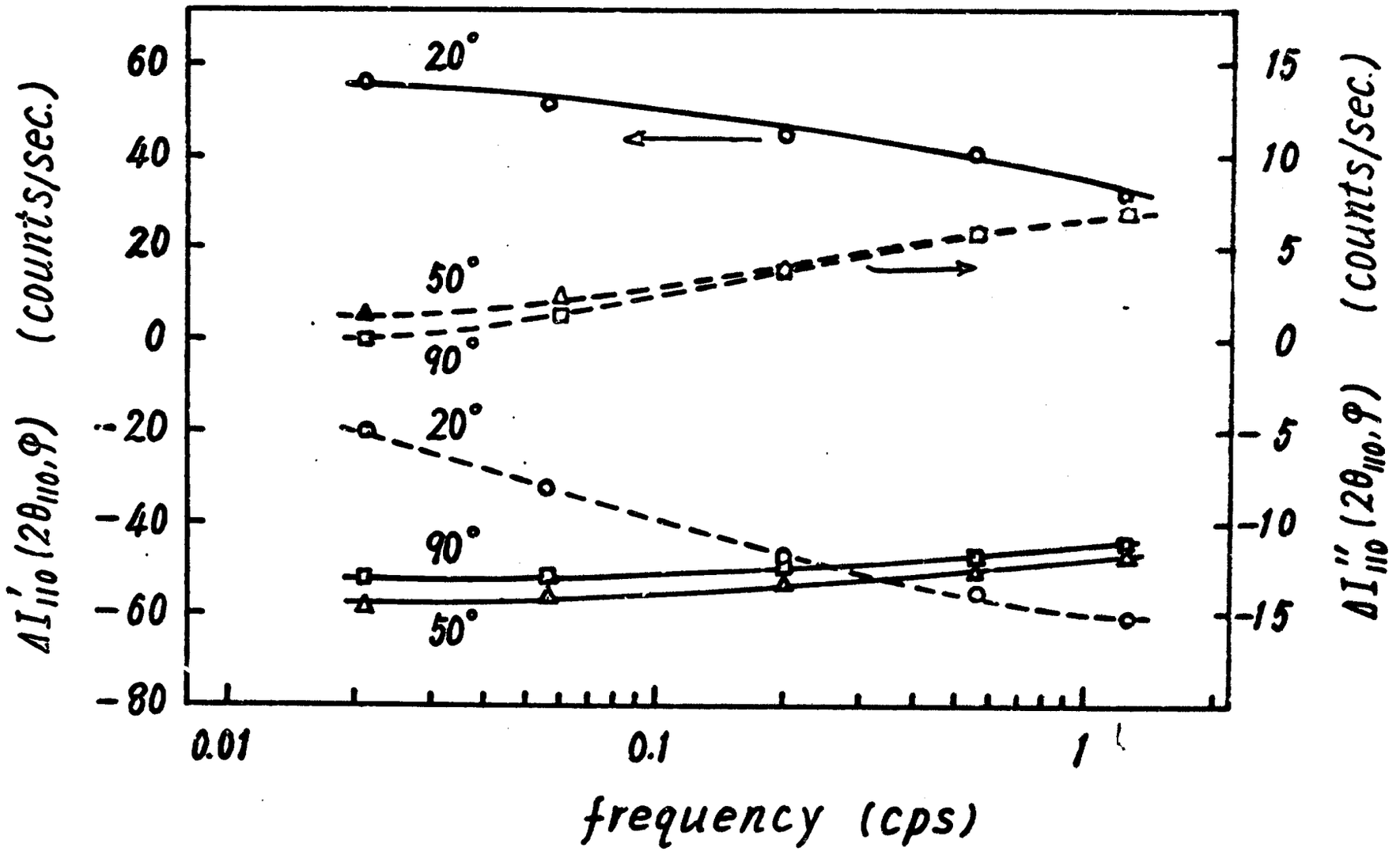
60
40
20
0
-20
-40
-60
-80
15
10
5
0
-5
-10
-15
20°
50°
90°
20°
90°
50°
0.01
0.1
1
frequency (cps)
ΔI'110 (2θ110, φ) (counts/sec.)
ΔI''110 (2θ110, φ) (counts/sec.)

FIGURE 8

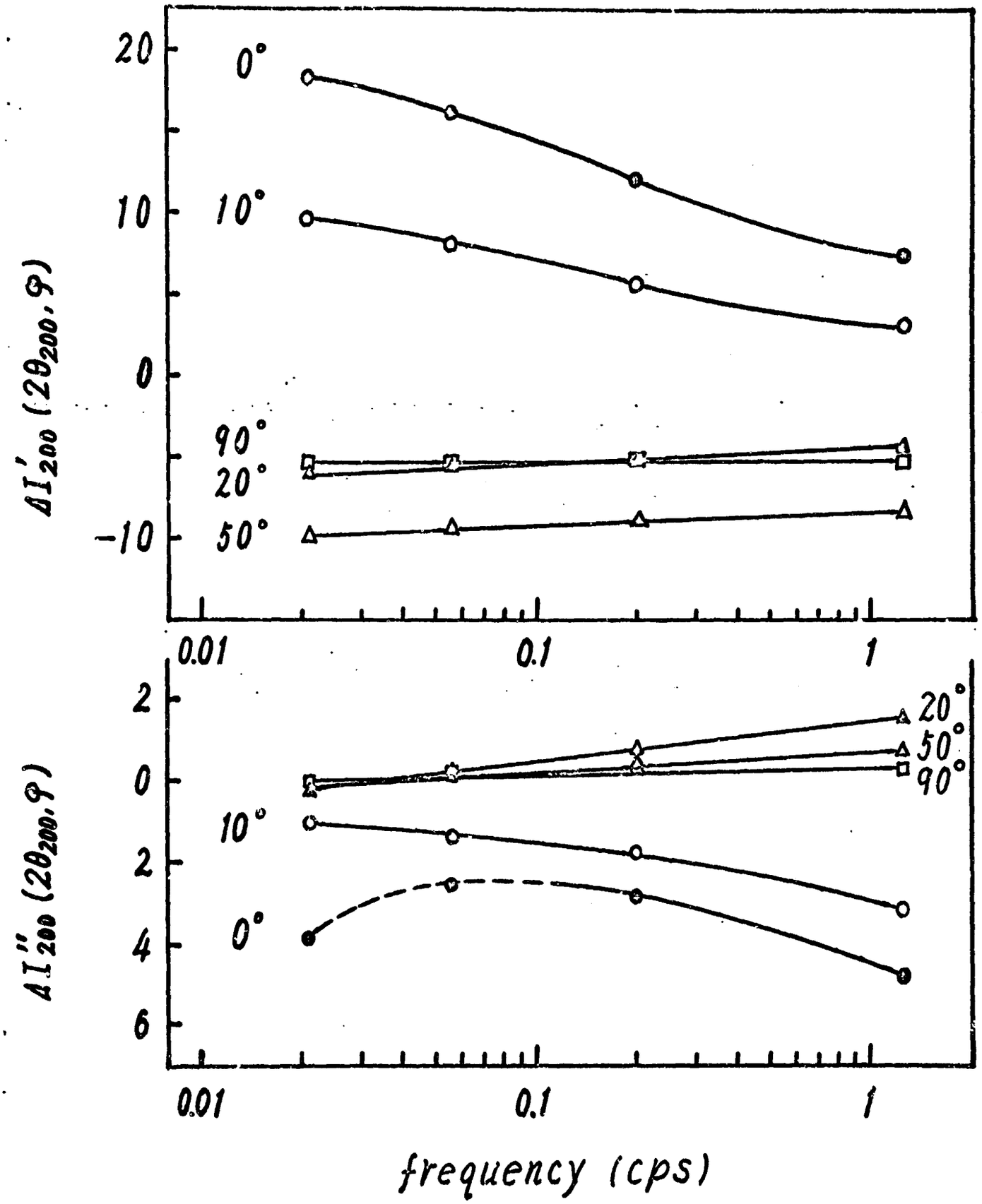
20
10
0
-10
0°
10°
90°
20°
50°
$\Delta I'_{200}(2\theta_{200}, \varphi)$
0.01
0.1
1
2
0
2
4
6
20°
50°
90°
10°
0°
$\Delta I''_{200}(2\theta_{200}, \varphi)$
0.01
0.1
1
frequency (cps)

FIGURE 9

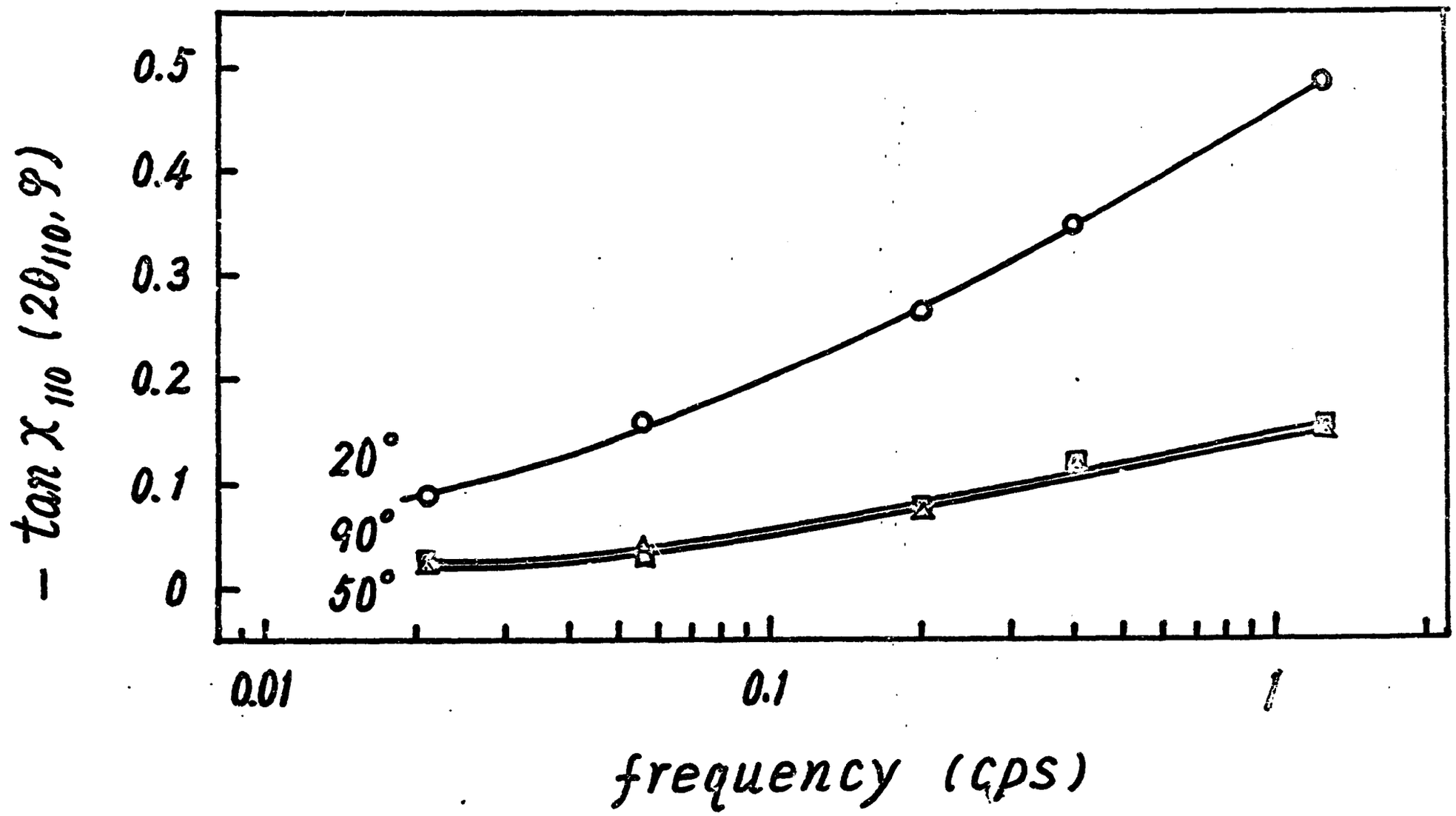
0.5
0.4
0.3
0.2
0.1
0
$-\tan \chi_{110}\,(2\theta_{110}, \varphi)$
20°
90°
50°
0.01
0.1
1
frequency (cps)

FIGURE 10

FIGURE 11

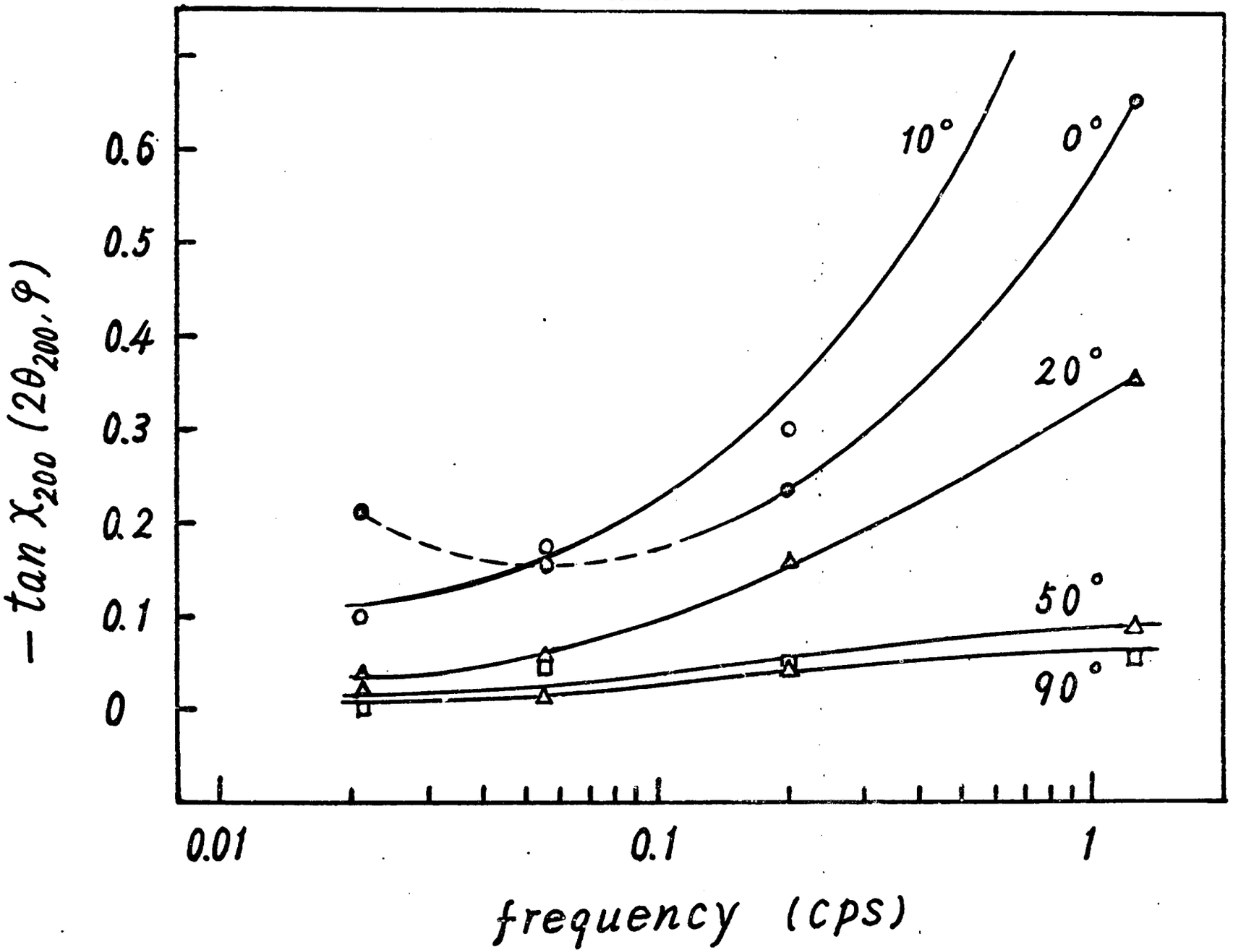
0.6
0.5
0.4
0.3
0.2
0.1
0
$-\tan \chi_{200}\,(2\theta_{200}, \varphi)$
10°
0°
20°
50°
90°
0.01
0.1
1
frequency (CPS)

FIGURE 12

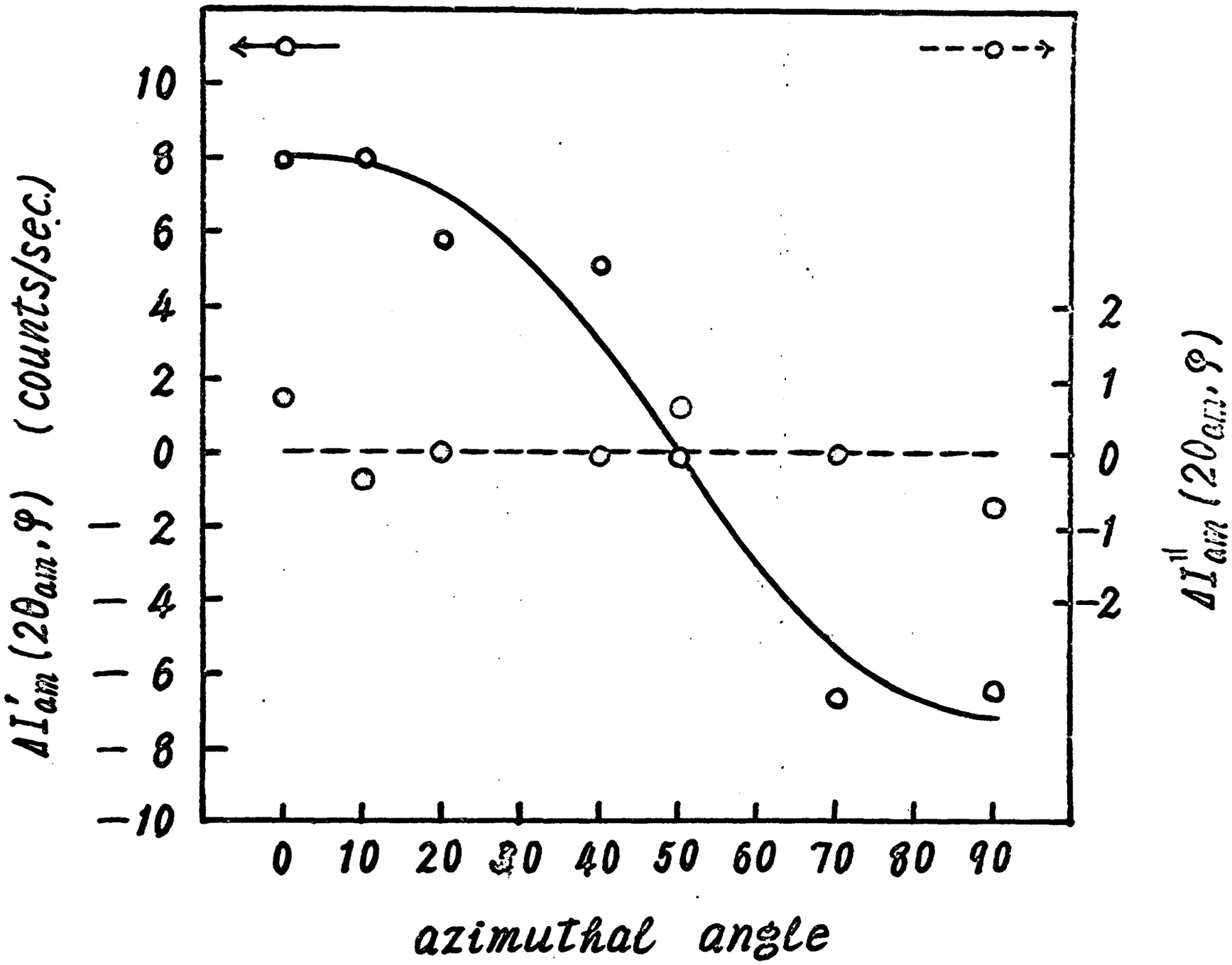
10
8
6
4
2
0
−2
−4
−6
−8
−10
0 10 20 30 40 50 60 70 80 90
azimuthal angle
$\Delta I'_{am}(2\theta_{am}, \varphi)$ (counts/sec.)
2
1
0
−1
−2
$\Delta I''_{am}(2\theta_{am}, \varphi)$

FIGURE 13

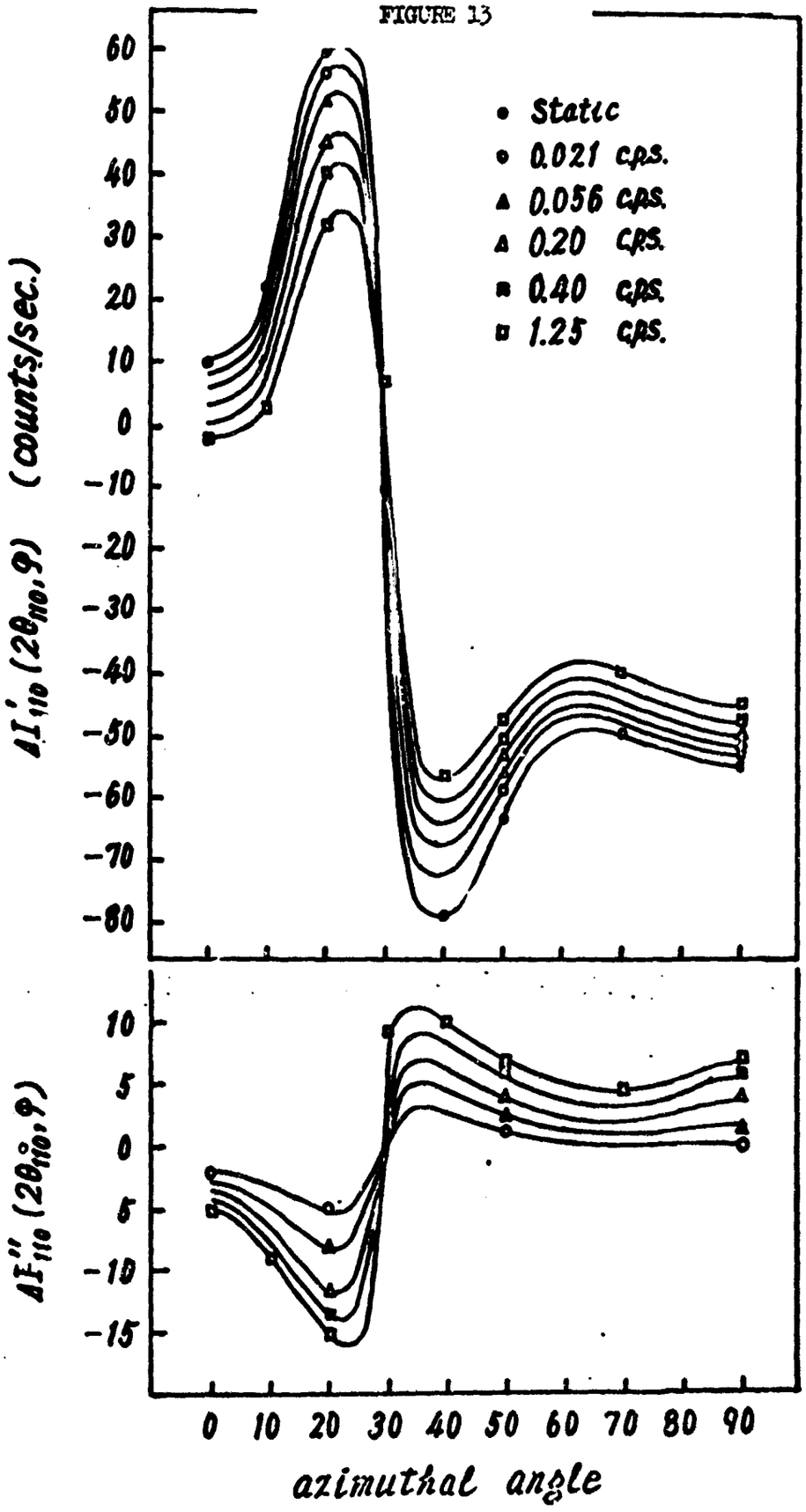
Static
0.021 c.p.s.
0.056 c.p.s.
0.20 c.p.s.
0.40 c.p.s.
1.25 c.p.s.
$\Delta I'_{110}(2\theta_{no},\varphi)$ (counts/sec.)
$\Delta I''_{110}(2\theta_{no},\varphi)$
azimuthal angle

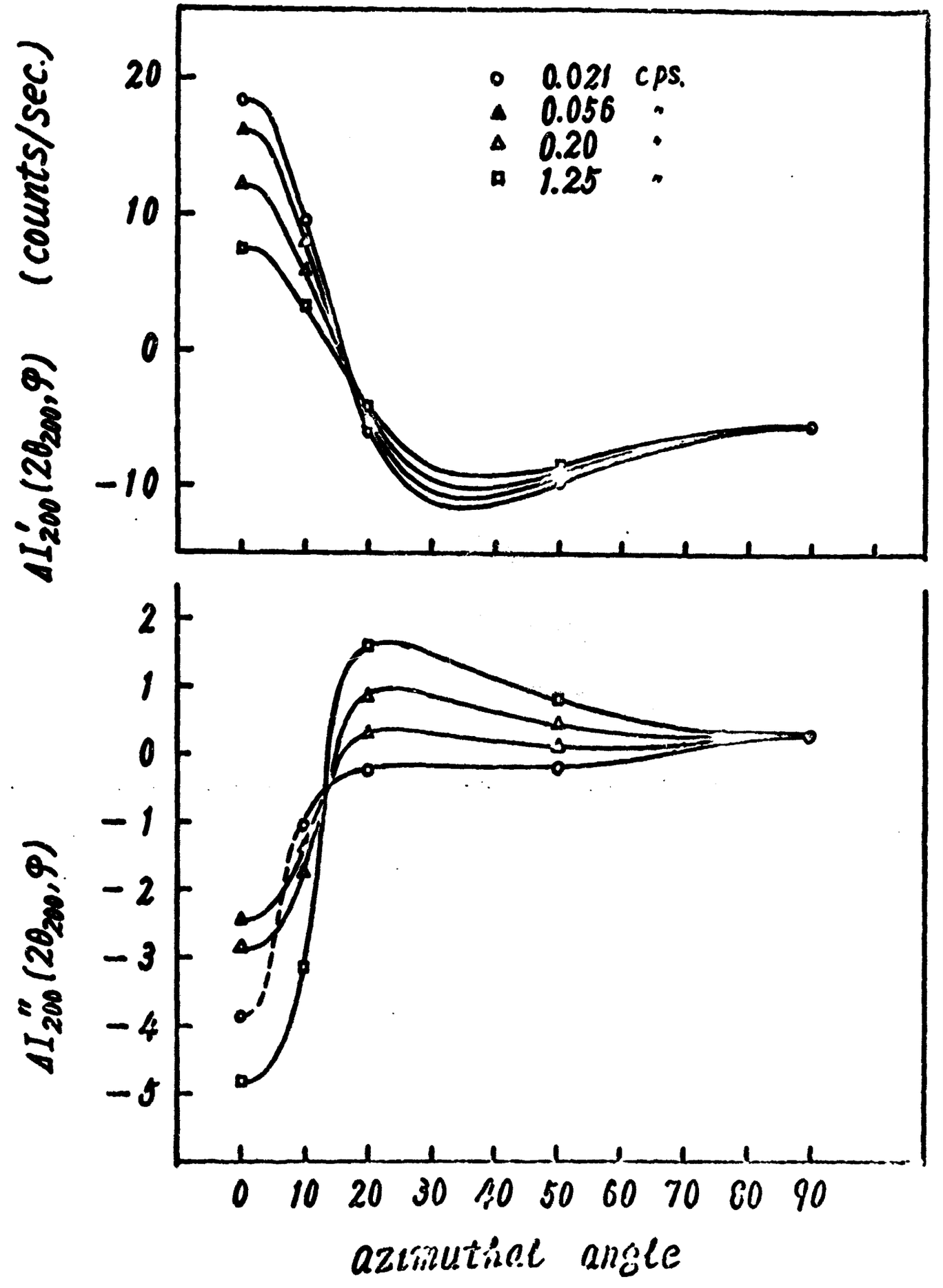
0.021 cps.
0.056 "
0.20 "
1.25 "
$\Delta I'_{200}(2\theta_{200},\varphi)$ (counts/sec.)
$\Delta I''_{200}(2\theta_{200},\varphi)$
azimuthal angle

FIGURE 3

FIGURE 15

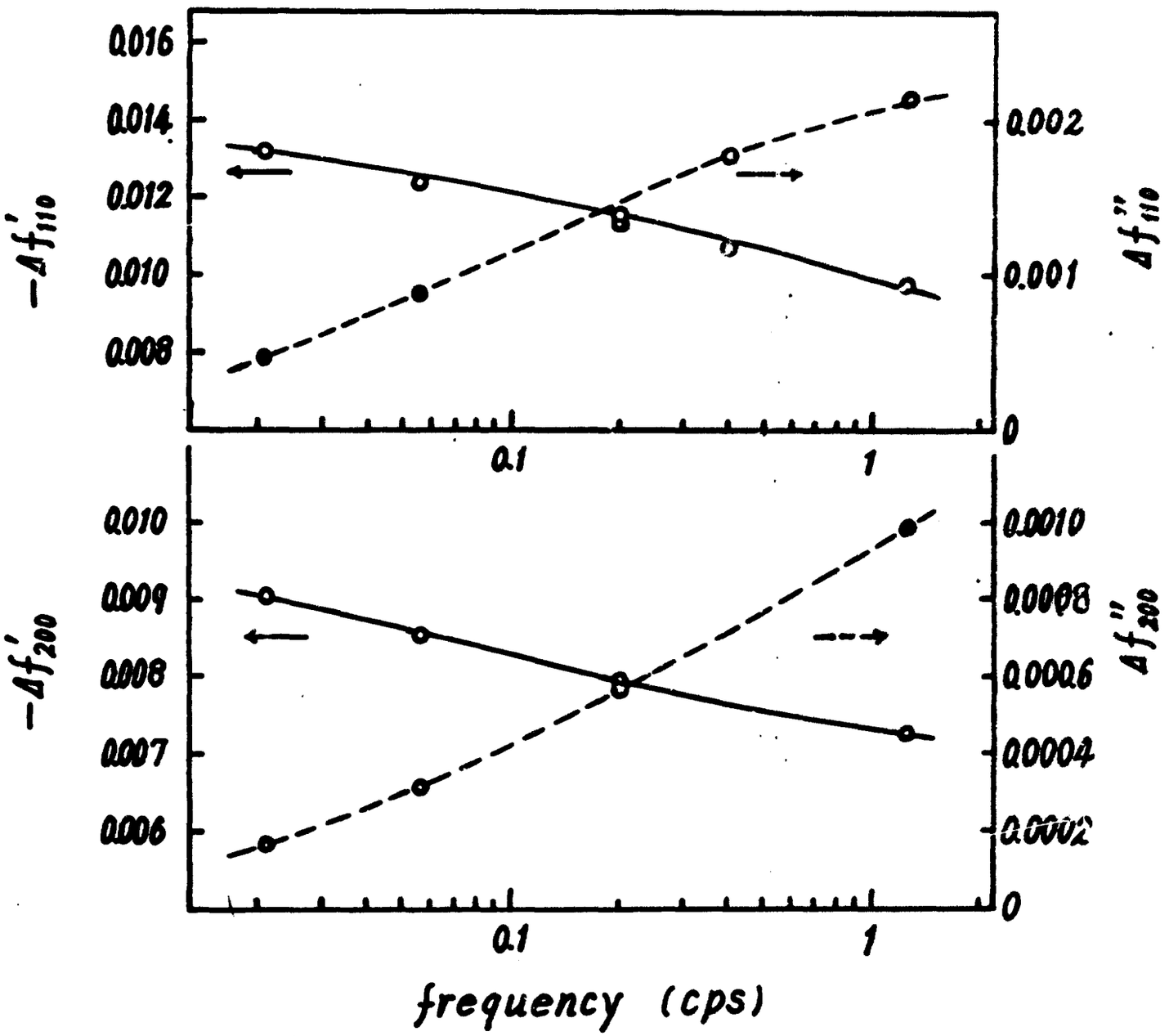
0.016
0.014
0.012
0.010
0.008
$-\Delta f'_{110}$
0.002
0.001
0
$\Delta f''_{110}$
0.1
1
0.010
0.009
0.008
0.007
0.006
$-\Delta f'_{200}$
0.0010
0.0008
0.0006
0.0004
0.0002
0
$\Delta f''_{200}$
0.1
1
frequency (cps)

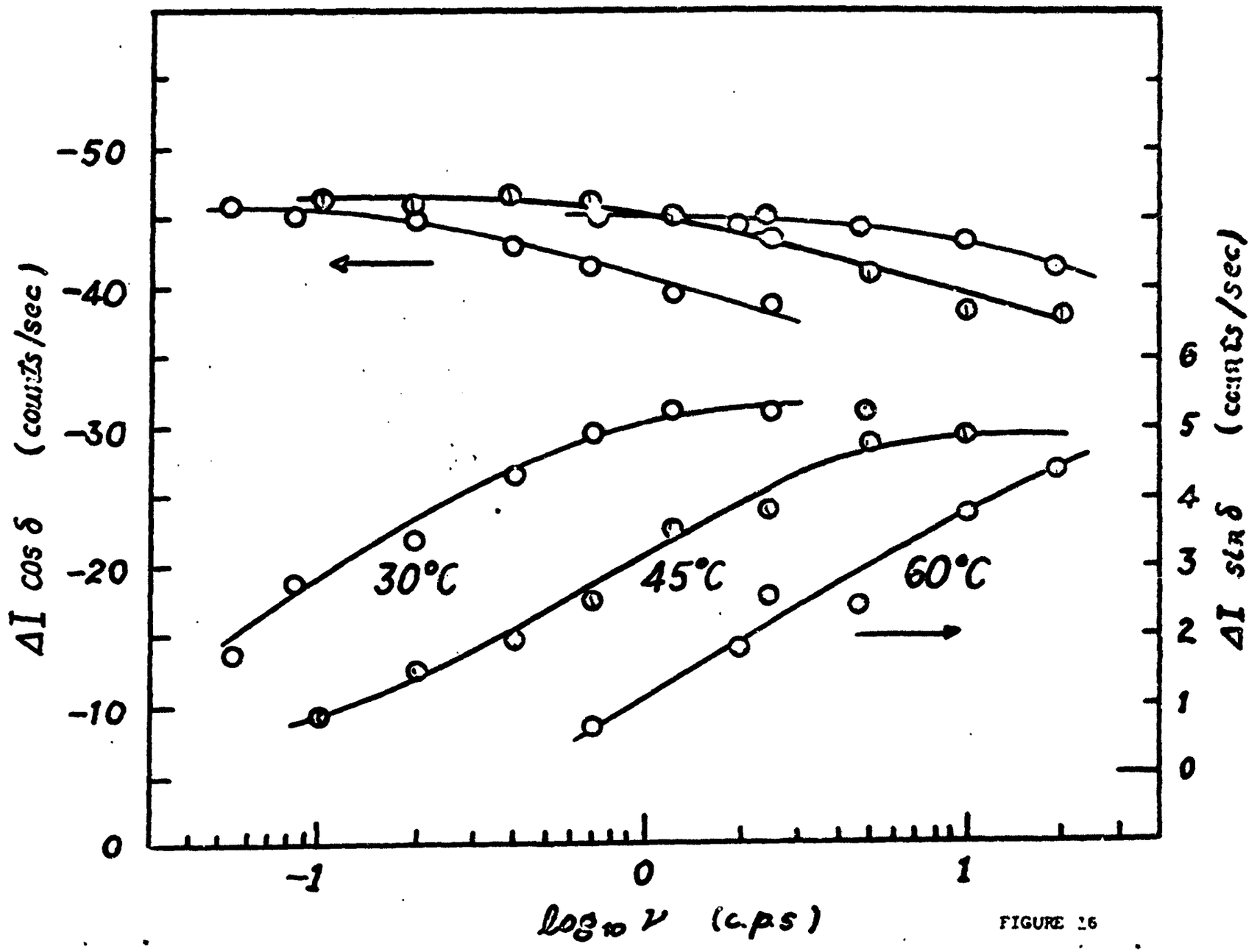
-50
-40
-30
-20
-10
0
ΔI cos δ (counts/sec)
30°C
45°C
60°C
6
5
4
3
2
1
0
ΔI sin δ (counts/sec)
-1
0
1
log10 ν (c.p.s)

FIGURE 16

log ν
-1
0
1
10000/T
30
31
32
33
34

Unclassified

Security Classification

DOCUMENT CONTROL DATA - R & D

Security classification of title, body of abstract and indexing annotation must be entered when the overall report is classified

1. ORIGINATING ACTIVITY (Corporate author)

Polymer Research Institute, Chemistry Department
University of Massachusetts, Amherst, Massachusetts

2a. REPORT SECURITY CLASSIFICATION

2b. GROUP

3. REPORT TITLE

Dynamic X-Ray Diffraction from Polyethylene

4. DESCRIPTIVE NOTES (Type of report and inclusive dates)

Technical Report

5. AUTHOR(S) (First name, middle initial, last name)

Tatsuro Kawaguchi, Taisuke Itoh, Hiromichi Kawai, Daniel Keedy and Richard S. Stein

6. REPORT DATE	7a. TOTAL NO. OF PAGES	7b. NO. OF REFS
November 1967	43	22

8a. CONTRACT OR GRANT NO	9a. ORIGINATOR'S REPORT NUMBER(S)
Nonr 3357(01)	97
b. PROJECT NO	
NR 056-378	
c	9b. OTHER REPORT NO(S) (Any other numbers that may be assigned this report)
d	

10. DISTRIBUTION STATEMENT

Qualified requesters may obtain copies of this report from the Polymer Research Institute, University of Massachusetts, Amherst, Massachusetts

11. SUPPLEMENTARY NOTES	12. SPONSORING MILITARY ACTIVITY
	Department of the Navy, Office of Naval Research, Boston Branch Office, 495 Summer Street, Boston, Massachusetts 02210

13. ABSTRACT

The technique of dynamic x-ray diffraction is described in which the periodically varying diffracted x-ray intensity is analyzed for a sample of a polymer film subjected to a periodic strain. The intensity change may be resolved into a real part, $\Delta I'$, varying in-phase with the strain and an imaginary out-of-phase component, $\Delta I''$. This resolution is carried out for the amorphous scattering and the diffraction from the {110} and {200} planes of medium density polyethylene at 30°C and at frequencies between 0.02 and 1.25 HZ. $\Delta I'$ decreases with frequency and $\Delta I''$ increases with frequency in the range as a consequence of a crystal orientation process having a relaxation time of the order of 1 sec. Measurements at temperatures of 30°, 45°, and 60°C produce a frequency shift associated with an activation energy of 25 Kcal/mole which is close to that for the α_2 process studied mechanically. By integrating the ΔI values over azimuthal angle it is possible to determine the real and imaginary parts of the dynamic orientation function, $\Delta f'$ and $\Delta f''$.

DD FORM 1 NOV 65 1473 (PAGE 1)

S/N 0101-807-6811

Unclassified

Security Classification